



Published in final edited form as:

Graefes Arch Clin Exp Ophthalmol. 2014 August ; 252(8): 1319–1327. doi:10.1007/s00417-014-2660-0.

Upregulation of hypoxia-inducible factors and autophagy in von Hippel-Lindau-associated retinal hemangioblastoma

Yujuan Wang^{1,2}, Mones S. Abu-Asab³, Defen Shen¹, Zhengping Zhuang⁴, Emily Y. Chew⁵, Chi-Chao Chan^{1,3}

¹Immunopathology Section, Laboratory of Immunology, National Eye Institute, National Institutes of Health, Bethesda, MD 20892, USA

²Zhongshan Ophthalmic Center, Sun Yat-sen University, Guangzhou 510060, China

³Histopathology Core, National Eye Institute, National Institutes of Health, Bethesda, MD 20892, USA

⁴Surgical Neurology Branch, National Institute of Neurological Disorders and Stroke, National Institutes of Health, Bethesda, MD 20892, USA

⁵Division of Epidemiology and Clinical Applications, National Eye Institute, National Institutes of Health, Bethesda, MD 20892, USA

Abstract

Purpose: To describe pathological and molecular changes of three patients with clinically severe von Hippel-Lindau (VHL)-associated retinal hemangioblastoma (RH) with rapid progression.

Methods: Medical records, ocular histopathology and transmission electron microscopy from three cases of VHL-associated RHs at the National Eye Institute were retrospectively reviewed. One eye of each patient was enucleated. Hypoxia-inducible factor (HIF) 1 α and HIF2 α expressions were identified by quantitative reverse transcription polymerase chain reaction (qRT-PCR) and immunohistochemistry.

Results: All three cases had rapidly growing RHs that were resistant to multiple conventional therapies and two (Patients 1 and 2) were also resistant to multiple intravitreal anti-vascular endothelial growth factor (VEGF) treatments. Macroscopically, all the enucleated eyes had multiple RHs, serous retinal detachment, severe retinal disorganization and focal hemorrhages. Histopathology showed typical RHs composed of vacuolated foamy von Hippel-Lindau cells and capillary networks. Retinal gliosis and hemorrhages were also presented. Additionally, T lymphocytes and macrophages were infiltrated in the tumors of two patients resistant to anti-VEGF therapy. Immunohistochemistry and qRT-PCR found upregulation of HIF1 α in the retinal lesions of all eyes. Importantly, upregulation of HIF2 α was exclusively detected in the two cases with inflammatory infiltration and resistance to anti-VEGF therapy. Ultrastructural images showed autophagy, lipid droplet, glycogen aggregations and cytoplasmic degeneration in many VHL cells.

Conclusions: Based on the histopathological and molecular pathological findings, autophagy, inflammation and/or upregulation of HIF2 α could potentially contribute to the aggressive course of RHs, resulting in the resistance to multiple anti-VEGF and radiation therapies in these patients.

Keywords

von Hippel-Lindau; retina; hemangioblastoma; hypoxia-inducible factors; autophagy; inflammation

Introduction

von Hippel-Lindau (VHL) disease is an autosomal dominant disease with an incidence of one in 36,000 live births [1]. It has multi-systemic tumors and affects the retina and central nervous system (CNS), as well as visceral organs, including the kidney, inner ear, pancreas, adrenal glands and epididymis at varying frequencies [2]. VHL is associated with a germline mutation of the *VHL* tumor suppressor gene on the chromosome 3p25 [3]. Loss of heterozygosity of *VHL* gene is well demonstrated in VHL-associated tumor cells including retinal and optic nerve head hemangioblastoma [4, 5]. VHL protein (pVHL) is encoded by *VHL* gene and acts to degrade the transcription factor called hypoxia-inducible factor (HIF). HIF is composed of α and β subunits and responds to changes in tissue oxygen concentration. HIF1 α and HIF2 α dimerize with constitutively expressed HIF1 β , also termed aryl hydrocarbon receptor nuclear translocator (ARNT), to activate the transcription of hypoxia-responsive genes. HIF2 α , also termed endothelial Per-Arnt-Sim (PAS) domain protein 1, is 48% identical in sequence to HIF1 α . Both HIF1 α and HIF2 α are inducible by hypoxia and associated with angiogenesis, glycolysis and apoptosis under hypoxic conditions [4, 6]. However, HIF1 α and HIF2 α are believed to have distinct functions, both in normal cellular physiology and in tumorigenesis [6–10].

Retinal hemangioblastoma (RH) is seen in 45-60% of VHL patients [11, 12], with two-thirds of them with multiple lesions [13] and bilateral in 26% of patients with VHL [14]. The ocular tumor appears typically as a round, globular reddish vascular lesion with a dilated feeding artery and a tortuous draining vein. It is found in either the juxtapapillary retina or the peripheral area. Although it usually has a benign nature and may be slow-growing, RH would disrupt retinal architecture or cause total retinal detachment, neovascular glaucoma, resulting in painful vision loss or even blindness in VHL patients. This is especially difficult when the tumor is located on or around the optic nerve as no known therapy is effective for this lesion. Early diagnosis and appropriate treatment reduce the risk of visual loss or blindness, especially for the lesions located peripherally. Several conventional methods have been used to ablate hemangioblastoma, including laser photocoagulation, cryotherapy, radiotherapy and photodynamic therapy. Recently, on the basis of molecular knowledge of tumorigenesis of VHL disease, some highly upregulated molecules, such as vascular endothelial growth factor (VEGF) and platelet-derived growth factor (PDGF), have been targeted in systemic and ocular VHL therapies [15].

Herein, we reported the pathological and molecular features of three enucleated eyes from three VHL patients with rapidly growing RHs that were refractory to therapy. In addition to

multiple VHL-associated RHs in the retina, we found upregulation of HIF1 α in all three patients with VHL-associated RHs. More importantly, the inflammatory infiltration and upregulation of HIF2 α are exclusively presented in two cases resistant to anti-VEGF therapy.

Materials and Methods

The study was approved by the National Eye Institute (NEI) Institutional Review Board for human subjects and an informed consent was signed by the patients. This study was conducted at the NEI and followed the tenets stated in the Declaration of Helsinki. Unilaterally enucleated eyes from three patients of VHL-associated RHs were submitted to NEI.

Clinical examinations

Clinical examinations of the three patients were performed by a NEI ophthalmologist (EYC) and three local ophthalmologists, respectively. Table 1 summarized the brief clinical findings in these three patients.

Histopathology

The enucleated eyes were fixed in 10% neutral buffered formalin for at least 24 hours before macroscopic and microscopic evaluation. The globes were cut horizontally through the macula along the pupillary-optic nerve head plane, where a VHL lesion was located. In areas of RHs, a segment through the lesion was also obtained for transmission electron microscopy (TEM). The grossed eyes were paraffin embedded and slides were stained with hematoxylin & eosin (H&E) and Periodic acid-Schiff (PAS). Immunohistochemistry staining (avidin-biotin complex method) was also performed with primary antibodies to the following antigens: CD68 (macrophage biomarker, 1:100, BD pharmingen, San Diego, CA, USA), CD45RO (mainly for T lymphocyte, 1:100, Dako, Carpinteria, CA, USA), CD3 (T lymphocyte biomarker, 1:100, Dako), CD20 (B lymphocyte biomarker, 1:40, Dako), glial fibrillary acidic protein (GFAP, 1:100, Dako), HIF1 α (1: 100, Sigma-Aldrich, St Louis, MO, USA) and HIF2 α (1:200, Novus Biologicals, Littleton, CO, USA).

TEM

The retina containing the lesion was double-fixed in 2.5% glutaraldehyde and osmium tetroxide (0.5%), dehydrated, and embedded in Spurr's epoxy resin. Ultrathin sections (90 nm) that include retinal VHL tumors were prepared and double-stained with uranyl acetate and lead citrate, and viewed using a JEOL JEM 1010 transmission electron microscope.

Microdissection and qRT-PCR

Microdissection was performed manually on uncovered, H&E stained glass slides [16–18]. Approximately equal numbers (~200) of cells from the juxtapapillary and peripheral RH areas were microdissected. The microdissected cells were subjected for qRT-PCR using the technique described previously [4, 5, 19]. Total RNA was isolated from RH cells using Arcturus Paradise RNA isolation kit (Molecular Devices., Sunnyvale, California, USA). Equal amounts of RNA were reverse transcribed with Superscript II RNase H Reverse

Transcriptase (Invitrogen, Grand Island, NY, USA) to cDNA. Quantitative reverse transcription polymerase chain reaction (qRT-PCR) was performed on the resulting cDNA using Brilliant SYBR Green QPCR Master Mix (Stratagene, La Jolla, CA, USA). The comparative cycle threshold (Ct) value method, representing log transformation, was used to establish relative quantification of the fold changes in gene expression using 7500 Real Time PCR System (Life Technologies Co. Carlsbad, CA, USA). β -actin was used as an internal control. Primers of β -actin, *HIF1A* and *HIF2A* were purchased from SABiosciences.

Mutational Analysis of *HIF2A*

Genomic DNA was extracted from tumor tissues obtained from the patients with the use of a NucleoSpin Tissue Kit (Macherey-Nagel). *HIF2A* exons were amplified by PCR assays. The primer sets for exon amplification have been described previously [20]. The DNA sequence of each exon was determined by forward and reverse sequencing.

Results

Patient 1

A 40-year-old Caucasian male had a history of systemic VHL disease, including RH, bilateral renal cell carcinoma, and brainstem VHL hemangioblastomas. The patient had VHL-associated RH diagnosed at age 15 (in 1986). His left eye had deteriorated and was eventually enucleated in 2003. His optic nerve head lesion of the right eye was treated with laser photocoagulation in 1993. This optic nerve tumor progressed, causing marked exudation that affected his vision with a decrease to 20/200 in 2004. His vision further deteriorated to 20/500 with increased retinal hard exudates in January 2005 (Fig. 1a). The patient was then enrolled in a trial of intravitreal ranibizumab at the NEI/National Institutes of Health (NIH). He received monthly intravitreal ranibizumab 0.5 mg. His vision had improved to 20/250 in April 2005, but declined to 20/400 in May 2005. Despite additional ranibizumab injections, his vision continued to deteriorate to 20/500 within a month. At the completion of the multiple injections of ranibizumab in August 2005, he developed additional small RHs in the macula in addition to the optic nerve head tumor. His vision was less than 20/500. In February 2006, external beam radiation therapy was given to the large optic nerve head RH and laser therapy to the small RHs. In spite of all the therapeutic regimens, his vision dropped to 20/800. In March 2010, he developed vitreous hemorrhages, serous retinal detachment and persistent lipid accumulation with multiple chorioretinal scars, in addition to RHs in the optic nerve head and retina (Fig. 1b). In May 2011, he developed rubeosis iridis with IOP of 12 mmHg. Multiple intravitreal injections of 1.25 mg of bevacizumab were administered for iris neovascularization. However, there was no response to the treatment and the rubeotic eye had barely light perception and the IOP was controlled with topical anti-glaucoma medication, Cosopt. Because of uncontrollable pain, the patient elected to enucleate the blind right eye in January 2012. The patient also had a history of kidney transplantation for his renal cell carcinoma and has been treated with immunosuppressants, including prednisone, CellCept (mycophenolate mofetil) and parpmune (sirolimus). His father had died with VHL complications.

Macroscopic examination showed a whitish mass with focal hemorrhages around the optic nerve head and several smaller yellow-whitish lesions in the peripapillary retina (Fig. 1c, d). There were thick pre-retinal fibrous tissues with areas of hemorrhages in the vitreous (Fig. 1c, d); the retina outside the mass was detached (Fig. 1c). Small round yellowish chorioretinal lesions and diffuse yellowish crystal lipid deposition were observed in the retina.

Microscopic examination disclosed a large RH located at the optic nerve head, extending to the nasal and temporal peripapillary retina and involving the entire neuroretina (Fig. 1e). The tumor was mainly composed of clear polygonal cells with small nuclei and finely reticulated or foamy cytoplasm. Focal tortuous, thin-walled, capillary-like vessels and small hemorrhages were intermingled in the RH. Within the RH, there were many small and large areas of cystic degeneration, some of which contained a few retinal pigment epithelium (RPE), pigment granules, fibrins, and/or erythrocytes. Some macrophages (CD68 positive, Fig. 1f) and T lymphocytes (CD45RO positive, Fig. 1g) infiltrates were visible in the RH, while B lymphocytes (CD20 positive) were rarely seen. The retina also showed degeneration, disorganization and gliosis (GFAP positive, Fig. 1h). Secondary exudative retinal detachment was noted in the retina adjacent to the hemangioblastoma. A large continuous chorioretinal adhesion with focal inflammatory choroidal infiltrates was also seen in the peripapillary retina. Several other small and large peripheral RHs with similar features involved the neuroretina. Many erythrocytes, scattered lymphocytes and pigment-laden macrophages were mixed with condensed vitreous strands.

Patient 2

A 40-year-old female had a history of visual changes when she was pregnant with her son in 2000. Her right eye presented with vascular lesions at the optic nerve head surrounding with lipid exudates. Her DNA testing was positive for VHL. In 2004, her vision had continued to decline in the right eye. In 2006, fundus examination showed increasing lipid exudates and focal retinal detachment temporal disc. At her annual VHL screening, she was detected to have a cystic lesion in the right kidney. She continued to have a “questionable” hemangioblastoma in her thoracic spinal cord (T4 and T5). Her son also tested positive for VHL. She received 14 ranibizumab injections from February 2005 to February 2006 as part of the intravitreal trial. Despite the treatment, her ocular lesions progressed to total retinal detachment, developed rubeosis iridis and early phthisis bulbi. The painful blind right eye was enucleated in 2009. A portion of the eye was submitted to NEI.

Macroscopic examination of the specimen showed retinal tumors, total retinal detachment as well as extremely disorganized macula and optic nerve head. Focal hemorrhages were also seen.

Microscopic examination showed rubeosis iridis. Small amount of hemorrhages and fibrins were seen in the vitreous. The retina was totally detached in a funnel shape. The retinal stock completely lost its normal architecture and was replaced by glial tissues. There were a few nodules formed by RH cells, fibroglial tissue, hemosiderin-laden pigmented macrophages, rare giant cells and small vessels. Scattered T lymphocyte (CD3 positive) and moderate macrophage (CD68 positive) infiltrates were visualized in the RHs and

disorganized retina, while B-lymphocytes (CD20 positive) were not seen. The temporal (funnel mouth) peripheral retina was barely recognized, closely attached to an organized blood and vitreous fibrovascular membrane. The nasal peripheral retina (funnel mouth) had slightly better retinal structure of gliosis (GFAP positive) and cystic degeneration. A small focal foamy cellular aggregation (RH) and scattered erythrocytes were observed.

Patient 3

A 35-year-old female with VHL diagnosed in 1983 had a history of enucleation of the left eye in 1991 and intracranial surgery in 1993. In 2004, she presented with a blind severely painful right eye in spite of conservative therapies. Ocular examination showed no view into the posterior segment of the right eye because of a dense cataract and rubeosis iridis. No anti-VEGF therapy was administered to this patient. The right eye became blind and was enucleated in 2004. The frozen eye was submitted to NEI.

Macroscopy showed that the retina containing several RHs and was totally detached and adherent to the posterior lens. The subretinal space was filled with orange-yellowish fluid. There was a thin layer of bony structure beneath the detached retina and the posterior choroid (inferior > superior). No optic disc was visible due to total retinal detachment.

Microscopy showed the total detached retina with barely visible architecture; degenerative cysts, gliosis (GFAP positive) and several isolated foci of vascular abnormalities were also seen. Some of these vascular abnormalities were typical VHL-associated RHs consisting of thin-walled, capillary-like or small hyalinized vascular walls forming an anastomosing pattern separated by a few plump, vacuolated cells. The other vascular abnormalities were mostly occluded hypocellular vascular structures. Areas of ghost erythrocytes and large cholesterol clefts were also present in the detached retina. Bone formation was noted in the subretinal tissue above and/or in the posterior choroid. Focal lymphocytic infiltration is seen in the choroid.

HIF1 α and HIF2 α expressions in RHs

HIF1A transcript detected by qRT-PCR was expressed in all retinas of the three patients, especially in Patients 1 and 2 (Fig. 2a). Similarly, HIF1 α protein was positively expressed in some VHL-associated RH cells of all retinas in the three patients (Fig. 2b, c, d). In contrast, *HIF2A* transcript expression was significantly higher in Patients 1 and 2, who had retinal inflammatory infiltration and were resistant to anti-VEGF therapy (Fig. 3a). HIF2 α protein was also abundant in the VHL-associated RH cells of these two patients compared to that in Patient 3 (Fig. 3b, c, d). *HIF2A* gene mutation was not detected in the tissues of all three patients.

Ultrastructure of RH

The viable VHL tumor cells appeared undifferentiated in the three cases. Most VHL-associated RH cells contained large vacuoles, degenerated cytoplasm and abnormal mitochondria (Fig. 4a, b). Some VHL cells contained autophagosomes, glycogen aggregations, lipid droplets and chromatin disintegration; and others appeared apoptotic (Fig. 4c, d). Activated glial cells were intermingled with VHL-associated RH cells.

Discussion

Our study provides molecular evidence that the VHL-associated RH cells express HIF2 α in two patients resistant to anti-VEGF therapy. Furthermore, histopathological findings identify the unusual presence of inflammatory infiltrates in the RH cells in these two patients. These suggest that high levels of HIF2 α could be another key element that is directly or indirectly associated with development of highly aggressive vascular tumors. Moreover, ultrastructural examination revealed the presence of autophagy, mitochondrial dysfunction, lipid metabolic abnormality and cytoplasmic degeneration in the RH cells. One or all of the pathological and molecular features of the patients may be associated with the refractory VHL clinical course and their resistance to multiple anti-VEGF and radiation therapies.

The pVHL encoded by the *VHL* gene is ubiquitously expressed and regulates the ubiquitination of HIF, thus marking it for degradation [21]. Under hypoxic conditions, intracellular levels of HIF are upregulated and result in increased expression of several proteins reversing hypoxia, such as erythropoietin, VEGF and PDGF [22]. Inactivation of VHL protein causes constitutive stabilization of HIF and ultimately leads to VHL-associated tumor progression. Our previous studies have already illustrated upregulation of VEGF in VHL-associated human RH specimens [4, 19]. Although VEGF is regulated by both HIF1 α and 2 α subunits, suppression of HIF2 α activity is thought to be more critical than HIF1 α activity for tumor suppression by pVHL [23, 24]. In *Vhl* deficient mouse liver, HIF2 α is the dominant HIF in the pathogenesis of VHL-associated vascular tumors [9]. Mouse embryos originating from *Hif2 α* deficient embryonic stem cells display severe vascular defects [25]. A significant correlation between high VEGF and HIF2 α protein levels was found in human neuroblastoma specimens and HIF2 α stabilization was detected in well-vascularized regions of the neuroblastoma patient specimens [26]. High HIF2 α protein levels have even been correlated with advanced clinical stage and high VEGF expression [26]. Recently, somatic mutations in *HIF2A* are reported in patients with paragangliomas or somatostatinomas together with polycythemia [27]. These mutations disrupt the prolyl hydroxylation domain (PHD) of *HIF2A* and abolish the modification by PHD, resulting in the decrease of VHL recognition and VHL-associated degradation, as well as the stabilization of HIF2 α [28].

In our current study, upregulation of HIF2 α protein without *HIF2A* mutation is specifically detected in the two patients who were resistant to anti-VEGF therapy. This result may indicate a feedback loop between HIF2 α and anti-VEGF therapy. That is, the VHL-associated RHs cause HIF2 α upregulation, which results in high VEGF expression. Consequently, these high VEGF expression tumors are resistant to anti-VEGF therapy, which in turn ends with even higher HIF2 α expression. Except for the potential contribution of anti-VEGF therapy, long-standing clinical course and combined secondary complications in these VHL patients could lead to upregulation of HIF2 α . The fact of upregulated HIF2 α also raises another question as whether its elevation would result in resistance of anti-VEGF therapy. However, there is no solid evidence that HIF2 α elevation would directly cause resistance of anti-VEGF therapy. The recent IVAN study has not found relationship between *HIF2A* SNP alteration and treatment responsiveness to VEGF inhibition in patients with neovascular age-related macular degeneration [29].

HIF2 α is not only a critical factor regulating erythropoiesis and neovascularization, but also involved in lipid homeostasis and glucose metabolism in the liver [30, 31]. Quantitative analysis of glycogen content in the adult mouse liver revealed that *Vhl* inactivation leads to abnormal glycogen accumulation in hepatocytes [30]. This is in agreement with our ultrastructural findings of glycogen particles in the RH cells. Additionally, Rankin et al. have found that HIF2 α activation in mouse hepatocytes suppresses lipid synthesis and fatty acid β -oxidation, and promotes lipid accumulation [31]. This could explain the presence of these lipid droplets in the VHL tumor cells.

In addition to the molecular upregulation of HIF2 α , ultrastructural abnormalities in the RH cells were also prevalent. Most VHL-associated RH cells revealed cytoplasmic degeneration, abnormal mitochondria, autophagy, and nuclear chromatin disintegration, some of these cellular damages could have resulted from radiation therapy. The finding of autophagy or apoptosis in the RH could be due to previous anti-VEGF and/or radiotherapy. Autophagy is a process of degradation and recycling of proteins and intracellular components in response to starvation or stress [32]. With its duality of function, autophagy could either promote cell survival under metabolic situation or cause cell death under stressed conditions [33]. It can even protect certain cancer cells against anticancer treatments by blocking the apoptotic pathway [32]. Based on the clinical findings and ultrastructural features, autophagy in the VHL-associated RHs might indicate a causative role, which promotes growth and progression of these RH cells and contributes to the tumor aggressiveness.

Macrophages and T lymphocytes were observed in the tumor areas in two patients (Patients 1 and 2) who had an aggressive course of the disease. Chronic inflammation, although mild, is an uncommon presentation in VHL-associated RHs. Although some studies show that systemic and local anti-VEGF treatment had anti-inflammatory effects [34–36], preventive VEGF inhibition has been reported to worsen inflammation in a mouse model of acute colitis [37]. Evidence has also demonstrated that tumor resistance to anti-VEGF therapy can accelerate myeloid cell infiltration, which is strongly associated with tumor hypoxia [38]. Myeloid cells can be attracted to regions of tumor hypoxia and play a role in mediating resistance to antiangiogenic therapy [39, 40]. Further investigation is needed to explore the effects of anti-VEGF therapy on the inflammatory cellular infiltration and tumor hypoxia in VHL-associated RHs. The potential role of anti-inflammatory therapy remains to be investigated.

Both ultrastructural and molecular findings demonstrate potential factors that may lead to the refractory course of VHL patients and resistance to both conventional and anti-VEGF therapies. Several antiangiogenic agents, such as SU5416 (inhibitor of VEGF receptor 2), bevacizumab, ranibizumab, pegaptanib (an aptamer inhibits VEGF isoform 165), have been attempted in several clinical trials. However, the general efficacy of antiangiogenic agents in VHL-associated RHs is uncertain and even unfavorable [15]. Our new finding of HIF2 α expression in the resistant RH cells suggests a novel therapeutic approach of targeting HIF2 α as an alternative therapy for VHL-associated RHs.

Disclosure/Conflict of Interest

The National Eye Institute Intramural Research Program supported the study.

The authors declare that they have no conflict of interest.

References

1. Maher ER, Iselius L, Yates JR, Littler M, Benjamin C, Harris R, Sampson J, Williams A, Ferguson-Smith MA, Morton N (1991) Von Hippel-Lindau disease: a genetic study. *J Med Genet* 28:443–447. [PubMed: 1895313]
2. Lonser RR, Glenn GM, Walther M, Chew EY, Libutti SK, Linehan WM, Oldfield EH (2003) von Hippel-Lindau disease. *Lancet* 361:2059–2067. [PubMed: 12814730]
3. Seizinger BR, Rouleau GA, Ozelius LJ, Lane AH, Farmer GE, Lamiell JM, Haines J, Yuen JW, Collins D, Majoor-Krakauer D, et al. (1988) Von Hippel-Lindau disease maps to the region of chromosome 3 associated with renal cell carcinoma. *Nature* 332:268–269. [PubMed: 2894613]
4. Chan CC, Vortmeyer AO, Chew EY, Green WR, Matteson DM, Shen DF, Linehan WM, Lubensky IA, Zhuang Z (1999) VHL gene deletion and enhanced VEGF gene expression detected in the stromal cells of retinal angioma. *Arch Ophthalmol* 117:625–630. [PubMed: 10326959]
5. Chan CC, Lee YS, Zhuang Z, Hackett J, Chew EY (2004) Von Hippel-Lindau gene deletion and expression of hypoxia-inducible factor and ubiquitin in optic nerve hemangioma. *Trans Am Ophthalmol Soc* 102:75–79; discussion 79–81. [PubMed: 15747747]
6. Hu CJ, Wang LY, Chodosh LA, Keith B, Simon MC (2003) Differential roles of hypoxia-inducible factor 1alpha (HIF-1alpha) and HIF-2alpha in hypoxic gene regulation. *Mol Cell Biol* 23:9361–9374. [PubMed: 14645546]
7. Wang V, Davis DA, Haque M, Huang LE, Yarchoan R (2005) Differential gene up-regulation by hypoxia-inducible factor-1alpha and hypoxia-inducible factor-2alpha in HEK293T cells. *Cancer Res* 65:3299–3306. [PubMed: 15833863]
8. Lofstedt T, Fredlund E, Holmquist-Mengelbier L, Pietras A, Ovenberger M, Poellinger L, Pahlman S (2007) Hypoxia inducible factor-2alpha in cancer. *Cell Cycle* 6:919–926. [PubMed: 17404509]
9. Rankin EB, Rha J, Unger TL, Wu CH, Shutt HP, Johnson RS, Simon MC, Keith B, Haase VH (2008) Hypoxia-inducible factor-2 regulates vascular tumorigenesis in mice. *Oncogene* 27:5354–5358. [PubMed: 18490920]
10. Imamura T, Kikuchi H, Herraiz MT, Park DY, Mizukami Y, Mino-Kenduson M, Lynch MP, Rueda BR, Benita Y, Xavier RJ, Chung DC (2009) HIF-1alpha and HIF-2alpha have divergent roles in colon cancer. *Int J Cancer* 124:763–771. [PubMed: 19030186]
11. Webster AR, Maher ER, Moore AT (1999) Clinical characteristics of ocular angiomatosis in von Hippel-Lindau disease and correlation with germline mutation. *Arch Ophthalmol* 117:371–378. [PubMed: 10088816]
12. Dollfus H, Massin P, Taupin P, Nemeth C, Amara S, Giraud S, Beroud C, Dureau P, Gaudric A, Landais P, Richard S (2002) Retinal hemangioblastoma in von Hippel-Lindau disease: a clinical and molecular study. *Invest Ophthalmol Vis Sci* 43:3067–3074. [PubMed: 12202531]
13. Annesley WH Jr., Leonard BC, Shields JA, Tasman WS (1977) Fifteen year review of treated cases of retinal angiomatosis. *Trans Sect Ophthalmol Am Acad Ophthalmol Otolaryngol* 83:OP446–453.
14. Singh AD, Nouri M, Shields CL, Shields JA, Perez N (2002) Treatment of retinal capillary hemangioma. *Ophthalmology* 109:1799–1806. [PubMed: 12359597]
15. Wong WT, Chew EY (2008) Ocular von Hippel-Lindau disease: clinical update and emerging treatments. *Curr Opin Ophthalmol* 19:213–217. [PubMed: 18408496]
16. Shen DF, Zhuang Z, LeHoang P, Boni R, Zheng S, Nussenblatt RB, Chan CC (1998) Utility of microdissection and polymerase chain reaction for the detection of immunoglobulin gene rearrangement and translocation in primary intraocular lymphoma. *Ophthalmology* 105:1664–1669. [PubMed: 9754175]

17. Zhuang Z, Bertheau P, Emmert-Buck MR, Liotta LA, Gnarr J, Linehan WM, Lubensky IA (1995) A microdissection technique for archival DNA analysis of specific cell populations in lesions < 1 mm in size. *Am J Pathol* 146:620–625. [PubMed: 7887444]
18. Chan CC (2003) Molecular pathology of primary intraocular lymphoma. *Trans Am Ophthalmol Soc* 101:275–292. [PubMed: 14971583]
19. Liang X, Shen D, Huang Y, Yin C, Bojanowski CM, Zhuang Z, Chan CC (2007) Molecular pathology and CXCR4 expression in surgically excised retinal hemangioblastomas associated with von Hippel-Lindau disease. *Ophthalmology* 114:147–156. [PubMed: 17070589]
20. Morris MR, Hughes DJ, Tian YM, Ricketts CJ, Lau KW, Gentle D, Shuib S, Serrano-Fernandez P, Lubinski J, Wiesener MS, Pugh CW, Latif F, Ratcliffe PJ, Maher ER (2009) Mutation analysis of hypoxia-inducible factors HIF1A and HIF2A in renal cell carcinoma. *Anticancer Res* 29:4337–4343. [PubMed: 20032376]
21. Kaelin WG Jr. (2008) The von Hippel-Lindau tumour suppressor protein: O₂ sensing and cancer. *Nat Rev Cancer* 8:865–873. [PubMed: 18923434]
22. Semenza GL (1999) Regulation of mammalian O₂ homeostasis by hypoxia-inducible factor 1. *Annu Rev Cell Dev Biol* 15:551–578. [PubMed: 10611972]
23. Maranchie JK, Vasselli JR, Riss J, Bonifacino JS, Linehan WM, Klausner RD (2002) The contribution of VHL substrate binding and HIF1-alpha to the phenotype of VHL loss in renal cell carcinoma. *Cancer Cell* 1:247–255. [PubMed: 12086861]
24. Kondo K, Klco J, Nakamura E, Lechpammer M, Kaelin WG, Jr. (2002) Inhibition of HIF is necessary for tumor suppression by the von Hippel-Lindau protein. *Cancer Cell* 1:237–246. [PubMed: 12086860]
25. Peng J, Zhang L, Drysdale L, Fong GH (2000) The transcription factor EPAS-1/hypoxia-inducible factor 2alpha plays an important role in vascular remodeling. *Proc Natl Acad Sci U S A* 97:8386–8391. [PubMed: 10880563]
26. Holmquist-Mengelbier L, Fredlund E, Lofstedt T, Noguera R, Navarro S, Nilsson H, Pietras A, Vallon-Christersson J, Borg A, Gradin K, Poellinger L, Pahlman S (2006) Recruitment of HIF-1alpha and HIF-2alpha to common target genes is differentially regulated in neuroblastoma: HIF-2alpha promotes an aggressive phenotype. *Cancer Cell* 10:413–423. [PubMed: 17097563]
27. Zhuang Z, Yang C, Lorenzo F, Merino M, Fojo T, Kebebew E, Popovic V, Stratakis CA, Prchal JT, Pacak K (2012) Somatic HIF2A gain-of-function mutations in paraganglioma with polycythemia. *N Engl J Med* 367:922–930. [PubMed: 22931260]
28. Yang C, Sun MG, Matro J, Huynh TT, Rahimpour S, Prchal JT, Lechan R, Lonser R, Pacak K, Zhuang Z (2013) Novel HIF2A mutations disrupt oxygen sensing, leading to polycythemia, paragangliomas, and somatostatinomas. *Blood* 121:2563–2566. [PubMed: 23361906]
29. Lotery AJ, Gibson J, Cree AJ, Downes SM, Harding SP, Rogers CA, Reeves BC, Ennis S, Chakravarthy U (2013) Pharmacogenetic associations with vascular endothelial growth factor inhibition in participants with neovascular age-related macular degeneration in the IVAN Study. *Ophthalmology* 120:2637–2643. [PubMed: 24070809]
30. Park SK, Haase VH, Johnson RS (2007) von Hippel Lindau tumor suppressor regulates hepatic glucose metabolism by controlling expression of glucose transporter 2 and glucose 6-phosphatase. *Int J Oncol* 30:341–348. [PubMed: 17203215]
31. Rankin EB, Rha J, Selak MA, Unger TL, Keith B, Liu Q, Haase VH (2009) Hypoxia-inducible factor 2 regulates hepatic lipid metabolism. *Mol Cell Biol* 29:4527–4538. [PubMed: 19528226]
32. Kondo Y, Kanzawa T, Sawaya R, Kondo S (2005) The role of autophagy in cancer development and response to therapy. *Nat Rev Cancer* 5:726–734. [PubMed: 16148885]
33. Turcotte S, Chan DA, Sutphin PD, Hay MP, Denny WA, Giaccia AJ (2008) A molecule targeting VHL-deficient renal cell carcinoma that induces autophagy. *Cancer Cell* 14:90–102. [PubMed: 18598947]
34. Schonhaler HB, Huggenberger R, Wculek SK, Detmar M, Wagner EF (2009) Systemic anti-VEGF treatment strongly reduces skin inflammation in a mouse model of psoriasis. *Proc Natl Acad Sci U S A* 106:21264–21269. [PubMed: 19995970]

35. Saravia M, Zapata G, Ferraiolo P, Racca L, Berra A (2009) Anti-VEGF monoclonal antibody-induced regression of corneal neovascularization and inflammation in a rabbit model of herpetic stromal keratitis. *Graefes Arch Clin Exp Ophthalmol* 247:1409–1416. [PubMed: 19655160]
36. Nakao S, Arima M, Ishikawa K, Kohno R, Kawahara S, Miyazaki M, Yoshida S, Enaida H, Hafezi-Moghadam A, Kono T, Ishibashi T (2012) Intravitreal anti-VEGF therapy blocks inflammatory cell infiltration and re-entry into the circulation in retinal angiogenesis. *Invest Ophthalmol Vis Sci* 53:4323–4328. [PubMed: 22661475]
37. Chernoguz A, Crawford K, Vandersall A, Rao M, Willson T, Denson LA, Frischer JS (2012) Pretreatment with anti-VEGF therapy may exacerbate inflammation in experimental acute colitis. *J Pediatr Surg* 47:347–354. [PubMed: 22325388]
38. Piao Y, Liang J, Holmes L, Zurita AJ, Henry V, Heymach JV, de Groot JF (2012) Glioblastoma resistance to anti-VEGF therapy is associated with myeloid cell infiltration, stem cell accumulation, and a mesenchymal phenotype. *Neuro Oncol* 14:1379–1392. [PubMed: 22965162]
39. Dirx AE, Oude Egbrink MG, Wagstaff J, Griffioen AW (2006) Monocyte/macrophage infiltration in tumors: modulators of angiogenesis. *J Leukoc Biol* 80:1183–1196. [PubMed: 16997855]
40. Murdoch C, Giannoudis A, Lewis CE (2004) Mechanisms regulating the recruitment of macrophages into hypoxic areas of tumors and other ischemic tissues. *Blood* 104:2224–2234. [PubMed: 15231578]

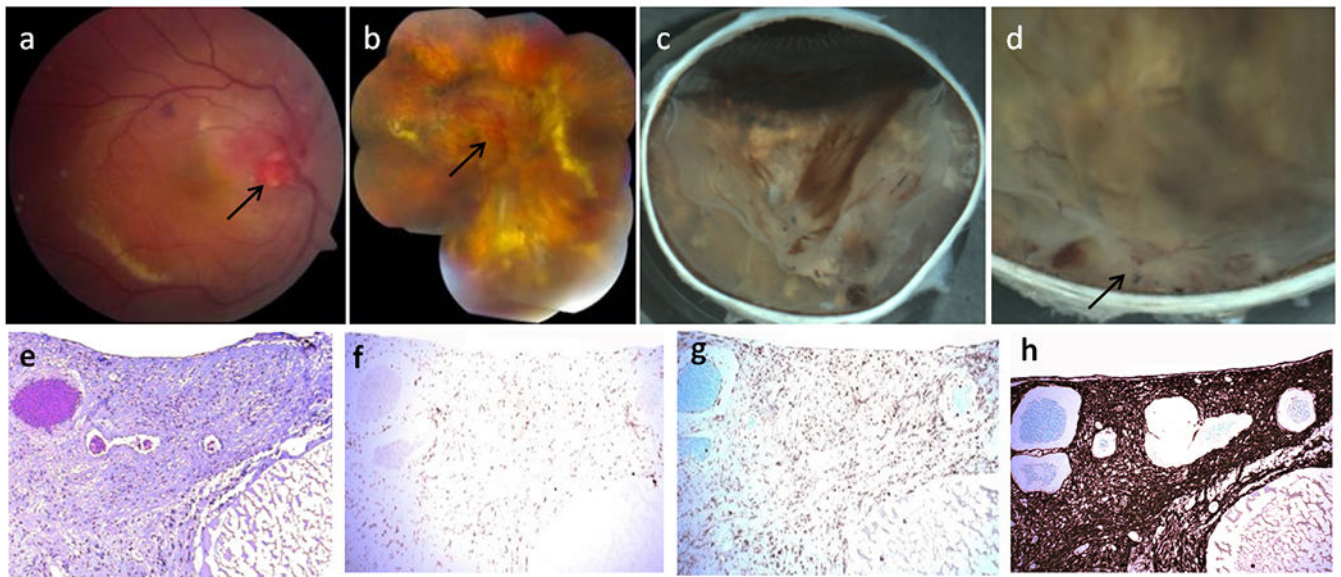


Fig. 1. Clinical photos and photomicrographs in Patient 1 with von Hippel-Lindau (VHL)-associated retinal hemangioblastoma (RH). Fundus photographs of VHL-associated RH in the right eye taken in January 2005 (a) and March 2010 (b). **a** The baseline fundus photograph before the intravitreal ranibizumab trial showed a prominent optic nerve tumor (arrow), focal hemorrhages and yellowish retinal hard exudates. **b** Ranibizumab and radiation therapy shows multiple vitreous hemorrhages, enlarged optic nerve tumor, serous retinal detachment, lipid accumulation and multiple pigmentary/yellowish chorioretinal lesions in the retina. Macroscopic photographs of VHL-associated RH in the right eye after enucleation in January 2012 (c, d). **c** The inferior calotte of the globe showed several patches of vitreous hemorrhages, yellowish chorioretinal lesions and retinal detachment. **d**. A whitish mass with focal hemorrhages around the optic nerve head (juxtapapillary RH) and several smaller lesions are observed in the peripapillary retina. **e** A large juxtapapillary RH was noted at the optic nerve head with a huge cyst (C) (hematoxylin and eosin (H&E) stain, original magnification, ×100). Avidin-biotin-complex immunohistochemistry staining corresponding to the same section with panel shows CD68 positive macrophages (f) and CD45RO positive T lymphocyte (g) infiltration in the juxtapapillary RH (original magnification, ×100). **h** Marked gliosis (glial fibrillary acidic protein positive) occurs in the whole areas of hemangioblastoma and retina (Avidin-biotin-complex immunohistochemistry, original magnification, ×200)

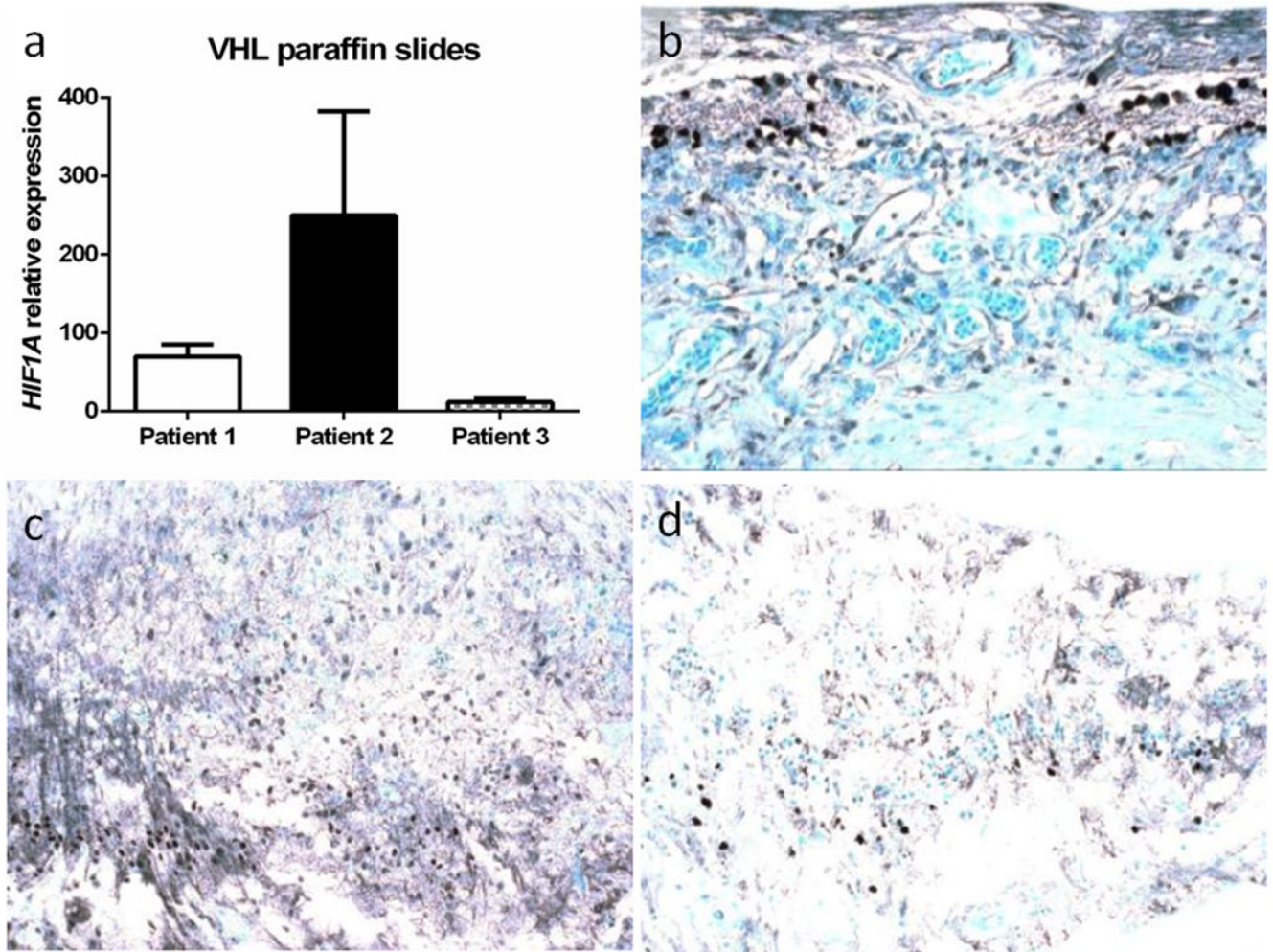


Fig. 2. HIF1 α expression in von Hippel-Lindau-associated retinal hemangioblastoma (RH) in 3 patients. **a** *HIF1A* transcript is comparably upregulated in the RH of 3 patients. Photomicrographs of HIF1 α protein expression in the RH cells in Patients 1 (**b**), 2 (**c**) and 3 (**d**) (Avidin-biotin-complex immunohistochemistry, original magnification, $\times 200$)

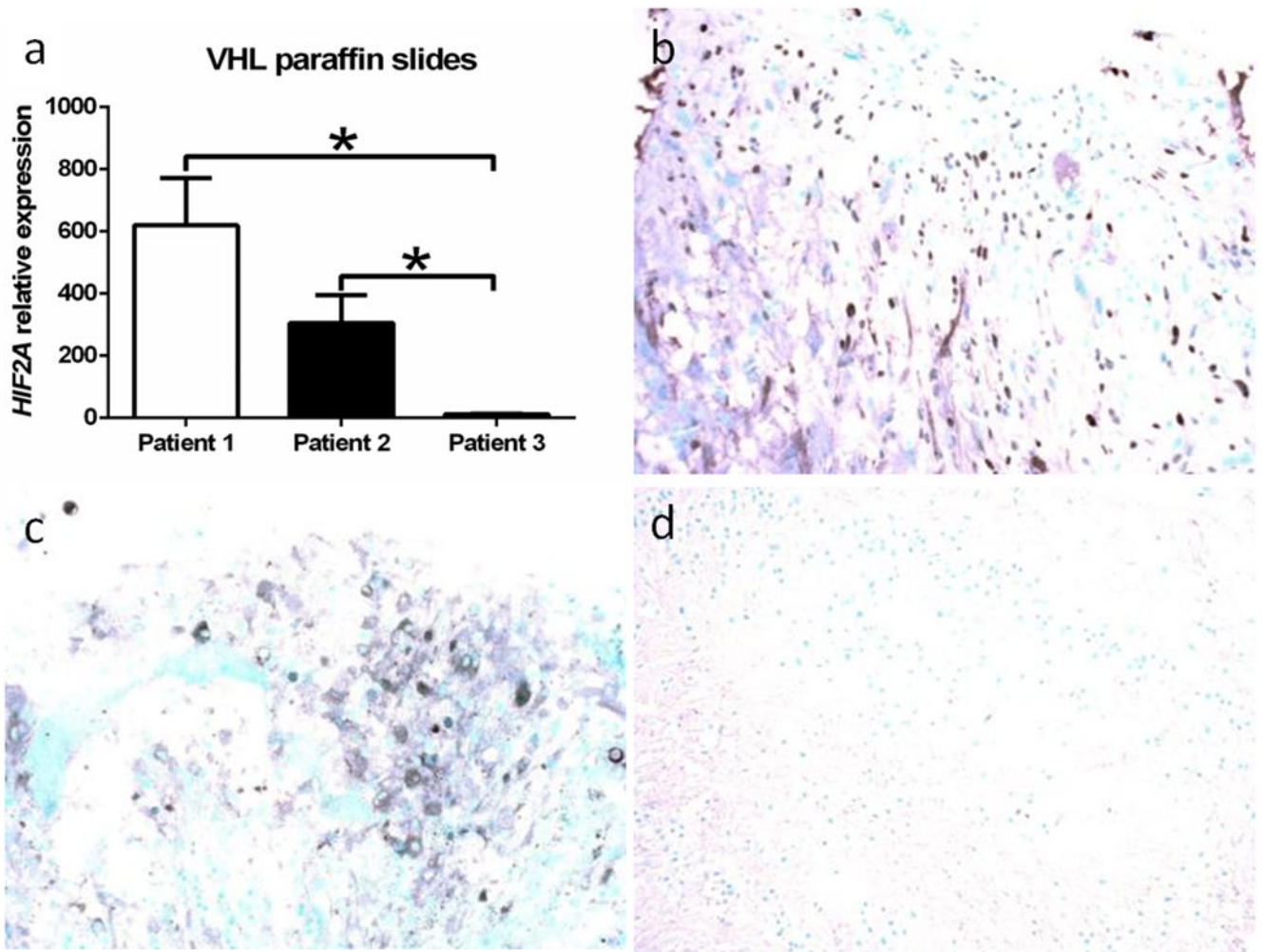


Fig. 3. HIF2 α expression in von Hippel-Lindau-associated retinal hemangioblastoma (RH). **a** *HIF2A* transcript expression is higher in the RH of Patients 1 and 2 than Patient 3. Photomicrographs of HIF2 α protein expression in the RH cells in Patient 1 (**b**) and Patient 2 (**c**), but not in Patient 3 (**d**) (Avidin-biotin-complex immunohistochemistry, original magnification, $\times 200$)

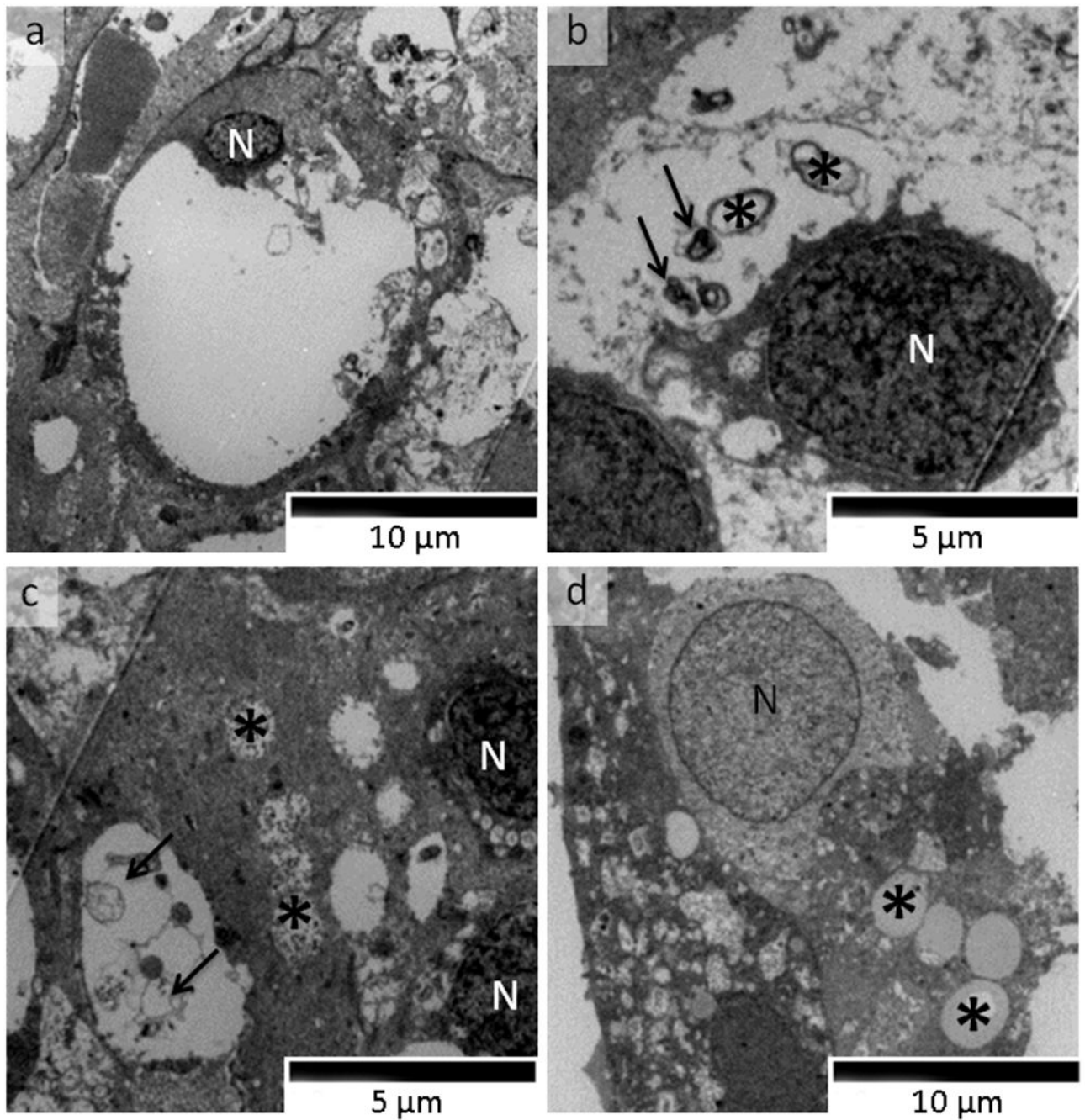


Fig. 4. Transmission electron microscopy photomicrograph of von Hippel-Lindau-associated retinal capillary hemangioblastoma (RH) cells of Patient 1 (original magnification, $\times 2500$). Ultrathin sections were prepared and double-stained with uranyl acetate and lead citrate. **a** A typical RH cell has degenerated cytoplasm and a small nucleus (N). **b** Degenerative cytoplasm autophagosomes (arrows) and damaged mitochondria (asterisks) in a RH cell (N, nucleus). **c** Glycogen aggregations (asterisks) and autophagosomes (arrows) are noted in RH

cells (N, nucleus). **d** Lipid droplets (asterisks) and nuclear chromatin disintegration are noted in a RH cell (N, nucleus)

Author Manuscript

Author Manuscript

Author Manuscript

Author Manuscript

Table 1

Brief summary of the clinical features in three VHL patients

	Patient 1	Patient 2	Patient 3
Age	40	40	35
Gender	Male	Female	Female
Systemic VHL involvement	Bilateral renal cell carcinoma and brainstem hemangioblastomas	Kidney cyst and Spinal cord hemangioblastoma (T4 and T5)	Brainstem hemangioblastoma Spinal cord hemangioblastoma (C6)
Duration of ocular VHL	25 years	9 years	21 years
Ocular VHL	One large juxtapapillary RH and several small peripheral RHs	One large juxtapapillary RH and several small peripheral RHs	Multiple small peripheral RHs
Therapies	Intravitreal anti-VEGF (ranibizumab and bevacizumab), laser photocoagulation and radiation	Intravitreal anti-VEGF (ranibizumab), laser photocoagulation and radiation	Laser photocoagulation and radiation, no anti-VEGF was administered
Enucleation	Left eye in 2003 Right eye in 2012 ^a	Right eye in 2009 ^a	Left eye in 1991 Right eye in 2004 ^a

^aThe enucleated eye presented in this study.